The EMBO Journal Vol.16 No.6 pp.1444–1454, 1997

A novel role of ImmE7 in the autoregulatory expression of the ColE7 operon and identification of possible RNase active sites in the crystal structure of dimeric ImmE7

Shih-Yang Hsieh, Tzu-Ping Ko[1], Ming-Yu Tseng, Wen-yen Ku[1,2], Kin-Fu Chak[3] and Hanna S.Yuan[1,3]

Institute of Biochemistry, Center for Cellular and Molecular Biology, National Yang Ming University, Shih-Pai, Taipei, Taiwan 11221, [1]Institute of Molecular Biology, Academia Sinica, Taipei, Taiwan 11529, [2]Graduate Institute of Life Sciences, National Defense Medical Center, Taipei, Taiwan, Republic of China

[3]Corresponding authors

S.-Y.Hsieh and T.-P.Ko contributed equally to this work

Site-specific cleavage of mRNA has been identified *in vivo* for the polycistronic colicin E7 operon (ColE7), which occurs between G and A nucleotides located at the Asp52 codon (GAT) of the immunity gene (*ceiE7*). *In vitro*, this specific cleavage occurs only in the presence of the *ceiE7* gene product (ImmE7). The crystal structure of dimeric ImmE7 has been determined at 1.8 Å resolution by X-ray crystallographic analysis. We found that several residues located at the interface of dimeric ImmE7 bear surprising resemblance to the active sites of some RNases. These results suggest that dimeric ImmE7 may possess a novel RNase activity that cleaves its own mRNA at a specific site and thus autoregulates translational expression of the downstream *celE7* gene as well as degradation of the upstream *ceaE7* mRNA.

Keywords: colicin E7 operon/dimeric ImmE7 structure/ immunity genes/RNase activity/site-specific cleavage

Introduction

The plasmid-encoded E group colicins bind to the vitamin B_{12} receptor (*btuB* gene product of *Escherichia coli*; DiMasi *et al.*, 1973) and have been subdivided by immunity tests into colicins E1–E9 (Watson *et al*., 1981; Cooper and James, 1984). The bactericidal activities of some E group colicins are well documented: colicin E1 exhibits an ionophore effect on the membrane of target cells (Tokuda and Konisky, 1979); colicin E3 is an RNase (Bowman *et al*., 1971); colicins E2 and E7–E9 are DNases (Schaller and Nomura, 1976; Toba *et al*., 1988; Chak *et al*., 1991).

Three genes, *cea*, *cei* and *cel*, located on the ColE operon are involved in colicin production, protecting colicin-producing cells against the action of their own colicin and release of the colicin–immunity protein complex respectively. Overexpression of the ColE operon is controlled by an SOS response promoter (Herschman and Helinski, 1967; Little and Mount, 1982). Lysis proteins (the *cel* gene product) among E group colicins may activate cell envelope phospholipase A and cause extensive damage to the cellular membrane (Pugsley and Schwartz, 1984). Thereby, overproduction of the *cel* gene can cause cell lysis. This 'suicidal phenomenon' arising from dramatic overexpression of the ColE operon has been compared with 'the programed cell death of bacteria' (Jensen and Gerdes, 1995; Yarmolinsky, 1995). To stabilize this 'killer system', coordinative expression of the ColE operon must be tightly controlled and efficient.

ImmE7 protein can bind to the endonuclease domain of ColE7 and neutralize its toxicity. The interaction between colicin and its cognate immunity protein is not only specific but is also the tightest among all known systems (Wallis *et al*., 1995a,b). Recently, the three-dimensional crystal structure of monomeric ImmE7 protein has been determined (Chak *et al*., 1996). It was suggested that the acidic protruding areas of ImmE7 may be involved in interacting with the basic T2A domain of colicin. From the present study, a specific endonucleolytic cleavage of the transcript has been found in the coding region of *ceiE7*. Using an *in vitro* transcription system, we observed that this specific endonucleolytic activity originated from ImmE7 itself. This observation was further supported by crystallographic analysis showing that the interface of dimeric ImmE7 presented possible RNase active sites similar to those of mammalian RNase A (Campbell and Petsko, 1987; Wlodawer *et al*., 1988) and some microbial RNases, including RNase Rh (Kurihara *et al*., 1992), barnase (Mauguen *et al*., 1982), RNase T1 (Koepke *et al*., 1989), RNase Sa (Sevcik *et al*., 1991), RNase F1 (Vassylyev *et al*., 1993) and RNase Ms (Nonaka *et al*., 1993).

This paper reports the novel ribonucleolytic activty of ImmE7 protein and its role in regulating expression of the ColE7 operon. The biological significance of the ColE7 operon coding a multifunctional ImmE7 protein is discussed.

Results

Measurement of the transcriptional strength across the junctions of the cea–cei–cel polycistronic transcript

Oligonucleotide primer design and the strategy for the reverse transcriptase (retrotherm reverse transcriptase) polymerase chain reaction (RT–PCR) are shown in Figure 1A. The oligonucleotide primer P4 is the common forward primer and primers P5, P1 and P2 are reverse primers. The PCR product (378 bp) amplified by oligonucleotide primers P4 and P5 represents the strength of transcriptional read-through from the *ceaE7* gene to the 5′-end of *ceiE7*; the 566 bp fragment indicates the strength of transcriptional read-through from *ceaE7* to the 3′-end of *ceiE7*. Similarly, the 757 bp PCR product shows the expression level from *ceaE7* to *celE7*.

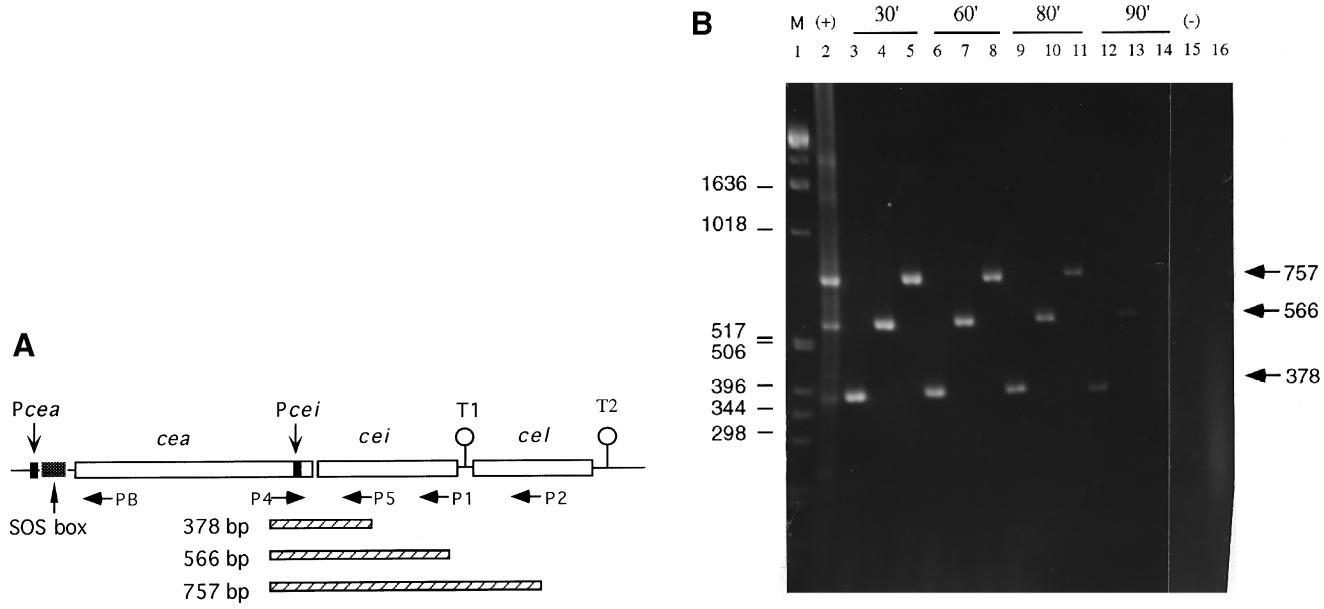

Fig. 1. Detection of the transcriptional strength across the junction of the ColE7 polycistronic transcript by RT–PCR analysis. (**A**) The strategy for RT–PCR amplification of the polycistronic transcripts from the ColE7 operon. Open bars represent the open reading frames of the ColE7 operon (Soong *et al*., 1991). Locations of the oligonucleotide primers, P1–P5, on the ColE7 operon are indicated. P4 is a common forward oligonucleotide primer and P2, P1 and P5 are reverse oligonucleotide primers for the detection of transcriptional strength at the designated junctions of the polycistronic transcript. PB is an oligonucleotide primer for the detection of transcriptional initiation sites of the ColE7 operon. The hatched bars represent the sizes of the PCR-amplified fragments. The relative position of the SOS box is also shown. P*cea* and P*cei* are the promoters of the *cea* and *cei* genes respectively. T1 and T2 indicate the relative locations of two putative hairpin structures of the operon. (**B**) Agarose gel electrophoresis of the RT–PCR amplified fragments. The RT–PCR products were analyzed by 3% agarose gel electrophoresis. At each time course, 20 μg total mRNA from W3110(pColE7) were used for RT–PCR analysis. 2.5 U retrotherm reverse transcriptase were used in a 50 μl reaction mixture for each reaction. After reaction, 15 μl RT–PCR product from each time interval were loaded onto a 3% agaorose gel. Lane 1, molecular mass markers. Lane 2, amplification of the 378, 566 and 757 bp fragments with ColE7 plasmid DNA as template, mixed P4, P5, P1 and P2 as primers and retrotherm reverse transcriptase as polymerase for the PCR. This amplification pattern was used as a reference. Lanes 3–14, RNA samples from the corresponding time points (30, 60, 80 and 90 min respectively) after mitomycin C (0.5 μg/ml) induction were amplified with retrotherm reverse transcriptase. Lanes 3, 6, 9 and 12, amplification patterns of the 378 bp fragment with P4 and P5 as primers; lanes 4, 7, 10 and 13, amplification pattern of the 566 bp fragment with P4 and P1 as primers; lanes 5, 8, 11 and 14, amplification pattern of the 757 bp fragment with P4 and P2 as primers. Lanes 15 and 16 are negative control panels. Lane 15, amplification of a RNA sample from the 90 min time point with Taq polymerase, instead of retrotherm reverse transcriptase, and P1, P2, P4 and P5 as mixed primers. Lane 16, RNA isolated from W3110(pUC18) amplified by retrotherm reverse transcriptase with P1, P2, P4 and P5 as mixed primers. Positions of the 378, 566 and 757 bp fragments on the agarose gel are indicated. + and –, positive and negative control panels respectively.

The results of PCR amplification of the DNA template from the ColE7 plasmid are shown in Figure 1B (lane 2). This positive control experiment indicated that the amplification intensity of the 757, 566 and 378 bp fragments were derived from the same copy number of DNA templates. Using this RT–PCR method to amplify the mRNA extracted from cells containing the ColE7 operon at different time intervals, we found that the intensities of these three fragments at the 30 min time point were similar (Figure 1B, lanes 3–5). Comparing the relative intensities of the RT–PCR products (Figure 1B, time intervals 30–90 min), it was found that the copy number of the target mRNA amplified by oligonucleotide primers P4 and P5 was far more than that of mRNA amplified by the other two sets of oligonucleotide primers. In contrast to the increase in promoter activity during induction (oligonucleotide primer PB as extension primer; data not shown), the quantities of mRNA produced from the RT–PCR products gradually decreased. Moreover, production for these three fragments appeared to be different. It was noticed that the amounts of the 566 and 757 bp fragments decreased faster than that of the 378 bp fragment. These unexpected patterns of amplification indicated that some unknown factor(s) may be involved in the regulation of copy number of mRNAs during induction. This phenomenon may most probably be due to post-transcriptional processing or decay of the polycistronic ColE7 mRNA.

Localization of site-specific cleavage of the ceiE7 transcript

To investigate the cause of the differential degradation rates of mRNA during induction, we performed primer extension with P1 as the extension oligonucleotide primer and *cei–cel* transcript as the template. Surprisingly, a 5′-end truncated transcript which terminated at a specific site between the G and A nucleotides of the Asp52 codon of *ceiE7* (Figure 2) was detected. This result was further confirmed by using oligonucleotide primer P2 for primer extension (data not shown). Neither primer P1 nor P2 could be used to detect the transcription initiation site for the *cei* gene (Figure 2). However, two transcription initiation sites (Soong *et al*., 1994) for the *cei* gene were detected when primer P5 was used. It seems most likely that breakage of the transcript at the Asp52 codon of the *ceiE7* transcript is indeed a specific cleavage site created after transcription. This specific cleavage was found under both non-induced and induced conditions (Figure 2). Furthermore, the accumulation of a larger amount of truncated *cei–cel* transcript coincided with an increase in transcriptional initiation at the SOS response promoter of

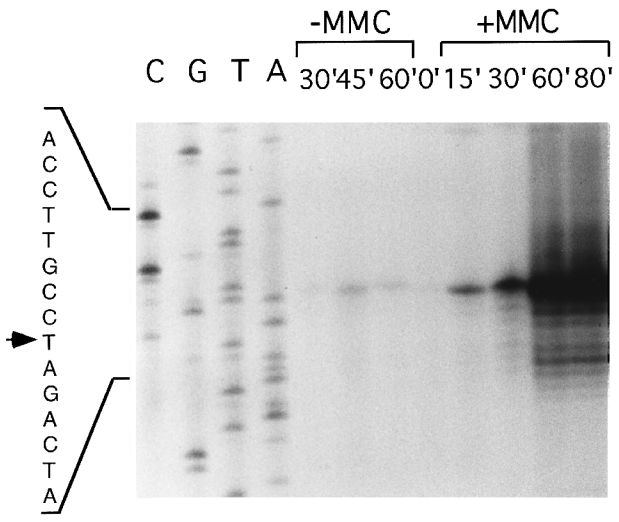

Fig. 2. Localization of the specific cleavage site of the *ceiE7* transcript. RNAs were prepared from cultures either with or without mitomycin C induction. Sampling time points for RNA preparation are indicated. A 40 μg RNA aliquot from each sample was used as template and primer P1 was used for both primer extension and nucleotide sequencing of the region. The method for primer extension is described in Materials and methods. Location of the specific cleavage site of the *ceiE7* transcript was identified by the sequencing ladder, which was run alongside the extension signals. An arrow indicates the location of the specific cleavage site of the *ceiE7* transcript. MMC, mitomycin C. + and –, with and without MMC induction respectively.

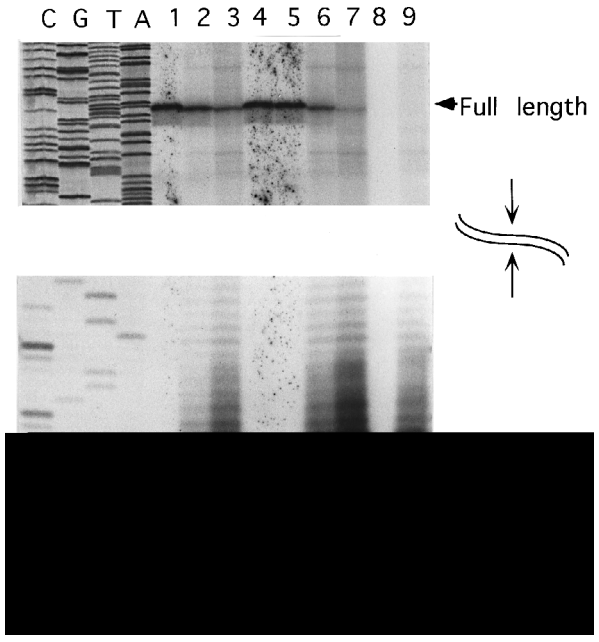

Fig. 3. ImmE7-dependent site-specific cleavage of *cei E7* mRNA. *In vitro* run-off *ceiE7* transcripts were prepared using the SP6 expression system. The 528 bp fragment as indicated was a full-length run-off transcript. Primer P1 was used both for primer extension and for nucleotide sequencing of the region. 100 ng SP6 promoter-transcribed RNA were used for each primer extension experiment. Lane 1, primer extension of the untreated run-off transcripts. Lanes 2–7, primer extensions of the run-off transcripts under different experimental conditions. Lanes 2 and 3, transcripts were treated with 0.3 μg purified ImmE7 for 5 or 10 min respectively; lane 4, transcripts were treated with 0.3 μg purified colicin E7; lane 5, transcripts were treated with 5 μl cell extract from *E.coli* JM109 containing pGEM3Z(f) for 30 min; lanes 6 and 7, transcripts were treated with 5 μl cell extract from *E.coli* JM109 containing plasmid pYAN13R (an expression vector containing the *ceiE7* gene for the preparation of run-off transcripts in this work) for 5 or 10 min respectively. Lanes 8 and 9, negative and positive controls. Lane 8, primer extension of 50 μg RNA prepared *in vivo* from *E.coli* W3110 containing pUC18. Lane 9, primer extension of 50 μg RNA prepared *in vivo* from *E.coli* W3110 containing pColE7. All primer extensions were performed in 20 μl reaction mixtures and 5 μl of each sample were loaded in each lane for electrophoresis. Since the positions of the full-length run-off transcripts and the truncated 3′-end transcripts on the sequencing gel are wide apart, for clarity only the top and bottom parts of the gel are shown.

the ColE7 operon (Soong *et al.*, 1994). Because of this specific cleavage, intact *cea–cei–cel* transcripts should be rare *in vivo* and can only be detected by a more sensitive RT–PCR amplification method (Figure 1, the 757 bp fragment).

Site-specific cleavage of the ceiE7 transcript is mediated by ImmE7 protein

RNase E and RNase III are the two most common endonucleases for degradation of RNA (for reviews see Belasco and Higgins, 1988; Higgins *et al*., 1992). However, the *ceiE7* mRNA extracted from RNase-deficient mutants (*Escherichia coli* N3433, N3431, RS6521 and SW001) carrying the ColE7 operon could not prevent the transcripts from being cleaved at the specific cleavage site (data not shown).

In vitro transcription was employed to study whether the specific cleavage occurred spontaneously or conditionally. When under the control of the SP6 promoter (Melton *et al.*, 1984), a full-length *ceiE7* run-off transcript (528 nt) initiated at the SP6 promoter was obtained (Figure 3). Specific cleavage was not observed under these *in vitro* conditions (Figure 3, lane 1). Specific cleavage was reproduced only if either purified ImmE7 or a crude extract from *E.coli* harboring a *ceiE7* gene was present in the assay system (Figure 3, lanes 2, 3, 6 and 7). These experimental results thus imply that the ImmE7 protein is required for this specific cleavage. Probably, ImmE7 exhibits a novel RNase activity to cleave its own transcripts at a specific site.

Crystal structure of dimeric ImmE7

The ImmE7 protein maintains an equilibrium between monomeric and dimeric forms that can be detected by chromatography (data not shown). This protein crystallizes in two distinct forms with the vapor diffusion method (Ku *et al.*, 1995). The monomeric ImmE7 structure was solved by the multiple isomorphous replacement method using orthorhombic crystals (Chak *et al*., 1996). Dimeric ImmE7 crystallizes in monoclinic space group $P2_1$ with cell dimensions a = 28.94 Å, b = 101.67 Å, c = 52.62 Å and β = 92.6°, indicating that four ImmE7 molecules are arranged in an asymmetric unit. The Matthew's coefficient (Matthews, 1968) would be 2.04 $Å^3$/Da and the estimated solvent content is 40%. The structure was solved by the molecular replacement method using the monomeric ImmE7 structure (Chak *et al.*, 1996) as searching model. Details of structure determination are described in Materials and methods.

The final model contains two dimeric pairs (M1/M3 and M2/M4) of ImmE7 with 2792 non-hydrogen atoms and 127 water molecules. The structure of the four individual molecules, M1, M2, M3 and M4, in the asym-

Table I. X-ray diffraction statistics for monoclinic ImmE7

Crystal size (mm×mm×mm)	0.5×0.3×0.1
Space group	$P2_1$
Unit cell dimensions	a = 28.9 Å
	b = 101.7 Å
	c = 52.6 Å
	$\alpha = \gamma = 90°$, $\beta = 92.6°$
Resolution (Å)	1.8
Molecules per asymmetric unit	4
Number of observed reflections	182 726
Number of unique reflections	28 088
Completeness (to 1.8 Å)	97.4%
R_{merge}[a]	6.3%
Number of non-hydrogen atoms	
All (including solvent molecules)	2919
Protein	2792
Solvent molecules	127
R factor (%) 6.0–1.8 Å	18.4
R_{free} (%)	26.8
r.m.s. deviation from standard geometry	
Bond lengths (Å)	0.020
Bond angles (°)	1.935
Average B factor (Å^2)	
For all non-hydrogen atoms	27.7
All protein atoms	27.5
Solvent atoms	32.9

[a]$R_{merge} = \Sigma_h\Sigma_i|I_{h,i}-\langle I_h\rangle|/\Sigma_h\Sigma_i I_{h,i}$, where $\langle I_h\rangle$ is the mean intensity of i observations for a given reflection h.

metric unit contains all of the 87 residues, which are numbered 101–187, 201–287, 301–387 and 401–487 respectively. Details of crystallographic statistics are listed in Table I. The Ramachandran plot (Ramakrishnan and Ramachandran, 1965) shows that all but three residues have ϕ, ψ angles out of the allowed range. The geometry was further checked by the program PROCHECK (Laskowski *et al*., 1993), in which 303 non-glycine residues (93.5%) are in the most favored area and 21 (6.5%) in allowed regions.

The backbone secondary structure of the dimer as assigned by PROCHECK is found to be identical to monomeric ImmE7 (Chak *et al*., 1996) in that they all consist of four anti-parallel α-helices: Helix 1 (12–25), Helix 2 (32–45), Helix 3 (52–55) and Helix 4 (65–78). In the monomeric structure, the N-terminal strand is parallel to Helix 2, however, in the dimeric structure, it is almost perpendicular to Helix 2. The 'open' conformation of the N-terminal strand helps to interlock the counter subunit in the dimeric structure (see Figure 4). The major interactions between the two ImmE7 molecules in a dimer involve Helix 2. The two helices propagate in opposite directions, with the nearest backbone atoms separated by 6.5 Å and an angle between the two Helices 2 of ~75°. Three residues, Val33, Val36 and Leu37, from each monomer are involved in hydrophobic contacts. These side chains form a hydrophobic core structure at the dimer interface. Surface areas of individual ImmE7 monomers range from 5538 to 5711 Å^2. The buried solvent-accessible surfaces for each molecule are 882 Å^2 for the dimer M1/M3 and 859 Å^2 for the dimer M2/M4 (calculated by Areamol in CCP4). A stable dimer of comparable molecular weight covers ~750 Å^2 (Janin *et al*., 1988), therefore, this dimeric ImmE7 structure should be stable in solution. In addition to the central hydrophobic core, residues Leu34, Leu38 and/or Val42 form a hydrophobic patch which may be responsible for docking the N-terminal strand of the counter monomer. Several acidic amino acid residues, Asp32, Asp35 and Glu39, located in the protruding area of Helix 1, Helix 2 and Variable Loop 2 of monomeric ImmE7 (Chak *et al*., 1996) were predicted to be involved in interaction with ColE7. In contrast, these residues are buried in dimeric ImmE7, indicating that interaction of dimeric ImmE7 with colicin seems impossible. This result suggests that dimeric ImmE7 could have some distinct biological functions other than inhibition of its cognate colicin.

The crystal structure of dimeric ImmE7 presents possible RNase active sites

The structures of RNase A and its complexes with various substrate analogs have established a mechanism for the hydrolysis reaction (Wodak *et al*., 1977; Nachman *et al*., 1990; Zegers *et al*., 1994). Three residues in the active site, His12, Lys41 and His119, of RNase A participate in the hydrolysis reaction. His12 and His119 are located on either side of the cleaved phosphate group and the amino group (NZ) of Lys41 lies in the vicinity of the ribose phosphate portion of the inhibitor. His12 behaves as a general base and substracts a proton from the 2′-OH group, whereas His119 acts as a general acid and furnishes a proton to the 5′-oxygen as it is being displaced from the phosphorus by nucleophilic attack of the 2′-oxygen atom. Lys41 forms a salt bridge with the negatively charged oxygen bound to the phosphorus and stabilizes the transition state.

By examining the structure of dimeric ImmE7, we found a pair of histidine residues (His40) which are located in the interface of the two subunits (Figure 4). His140 and His340 refer to the same His40 residue from different subunits (M1 and M3 respectively). The distance between the α-carbons of the two histidine residues, His140 and His340, is ~7 Å, compared with 9 Å for RNase A (His12 and His119). A lysine residue (Lys343) which is located close to the histidine residues is also found in ImmE7. Superimposition of the three residues (His12, His119 and Lys41 in RNase A and His340, His140 and Lys343 in ImmE7) by least squares fitting of the corresponding atoms gave an average r.m.s. deviation of only 1.20 Å. As shown in Figure 5A, when the active site of RNase A is superimposed on the proposed one of ImmE7, the imidazole rings of the histidines in the two enzymes can be overlapped in the same region by rotating the dihedral angle (C_α–C_β) of His140 by 120° in the ImmE7 structure. This rotation is allowed because it would not cause additional unfavorable Van der Waal's contacts. It has been shown that the general acid His119 in RNase A exhibits conformational mobility. By rotating about its C_α–C_β bond, the imidazole side chain can occupy two distinct conformations (Zegers *et al*., 1994). It is possible that the conformation of His40 in ImmE7 may change after binding to RNA.

The striking resemblance between RNase A and ImmE7 is not only found in the proteins, but also in their water structures. In the structure of phosphate-free RNase A (Wlodawer *et al*., 1988), two water molecules were found in the phosphate binding pocket. When compared with the structure of substrate-bound RNase A, one of the water molecules overlapped with the phosphate oxygen

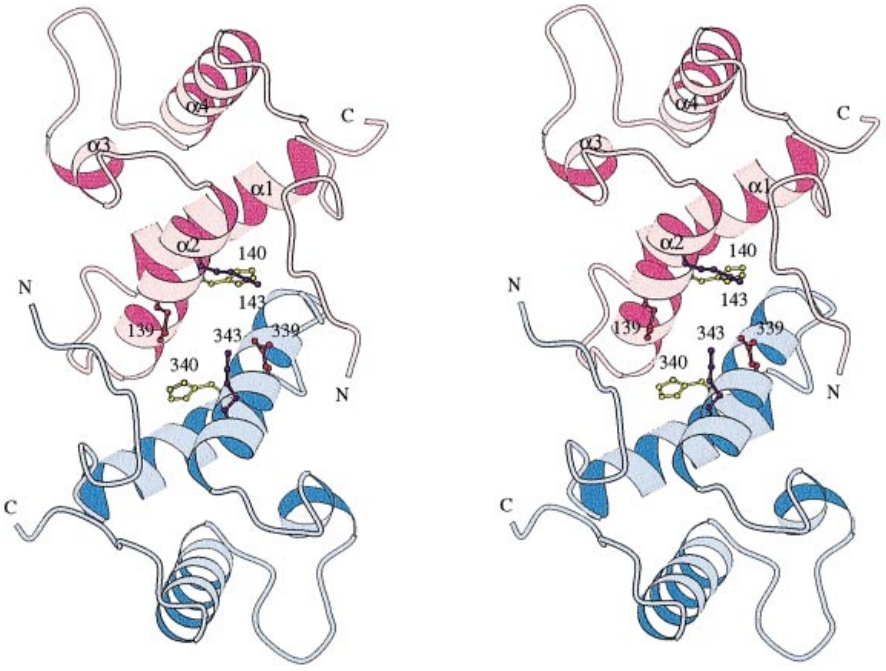

Fig. 4. Stereo views of the overall fold of dimeric ImmE7. The two subunits are colored pink and blue (M1 and M3) respectively. The four helices in the pink monomer are labeled α1–α4. The N-terminal tails are oriented in an 'open' conformation to interlock with the counter subunit. The residues possibly involved in the RNase active site are colored yellow for His40, blue for Lys43 and red for Glu39. His140 and His340 refer to the same His40 residues from subunits M1 and M3 respectively. The figure was prepared with MOLSCRIPT (Kraulis, 1991).

atom (near position O2). In dimeric ImmE7, there are also two water molecules located between the two histidine residues (see Figure 5A), indicating that His140 and His340 in dimeric ImmE7 could act as a general acid and base for RNase activity.

In addition to mammalian RNases, the structure of one enzyme, RNase Rh, in the larger microbial family has also been solved. The active site of RNase Rh (Kurihara *et al*., 1992) is similar to that of RNase A. Furthermore, study of a smaller family of microbial RNases suggested that a histidine and a glutamate are the general acid and base. These two residues in RNase Ms (Nonaka *et al*., 1993) nearly coincide with the His12 and His119 residues in RNase A. Despite the differences in their primary amino acid sequences and tertiary structural folding, there are similarities between mammalian RNase A and microbial RNases in the arrangement of the catalytic residues (Nonaka *et al*., 1993). These enzymes may have similar chemical mechanisms for phosphodiester hydrolysis.

In the vicinity of the active pocket we also find a nearby glutamate (Glu39) that could act as a general base, as observed in the smaller family of microbial RNases. It seems possible that the general acid and base of ImmE7 are a histidine and a glutamate from either monomer. As shown in Figure 5B, the residues His240, Glu439 and Lys243 of dimer M2/M4 overlap nicely with the corresponding residues of barnase. With distinct ImmE7 dimer pairs (Figure 5A and B) for comparison, it was demonstrated that the structures of the active sites in dimers M1/M3 and M2/M4 are identical. The average r.m.s. deviation between the corresponding atoms of the residues involved in the active site in barnase and ImmE7 is 1.43 Å.

The molecular surface of ImmE7 calculated using GRASP (Nicholls and Honig, 1991) shows a groove at the interface of dimeric ImmE7 between two adjacent Helices 2 (Figure 6A). A deep hole in the middle of the groove could be the binding site for the phosphate group and the two histidines are located exactly above and beneath the hole. Figure 6B shows a close-up of the proposed RNase active site in dimeric ImmE7, with the three residues His140, His340 and Lys343 located on the molecular surface, reachable by mRNA. There are several exposed basic residues located along the groove (Lys43, Lys81 and Arg76) (Figure 6A). Thus, this long groove in the dimeric interface could be the binding site for ribonucleic acids.

Site-specific cleavage of ceiE7 mRNA can regulate translational expression of the downstream celE7 transcript

celE7 is the third gene of the ColE7 operon and is promoterless (Chak and James, 1985; Chak *et al*., 1991). The regulation of expression of *celE7* is still unclear. It has been noted that not only is the translational stop codon of *ceiE7* located within the T1 stem–loop (Figure 7A), but also that the ribosome binding site of *celE7* is situated near the 3′-end of the T1 stem–loop structure (Figure 7A). Therefore, we speculate that cleavage of *ceiE7* mRNA may play an important role in the regulation of translational expression of *celE7* mRNA.

In order to investigate the regulation of *celE7* expression, three translational fusion mutants were generated. The recombinant plasmids, pHK001-13R, pHK001-14R and pSE4R, containing *lacZ* promoter–*ceiE7*–*celE7* fusions (Figure 7B), were constructed. pHK14R was an out-of-frame fusion mutant that created a new translational stop codon, UAG, 88 nt upstream of the original stop

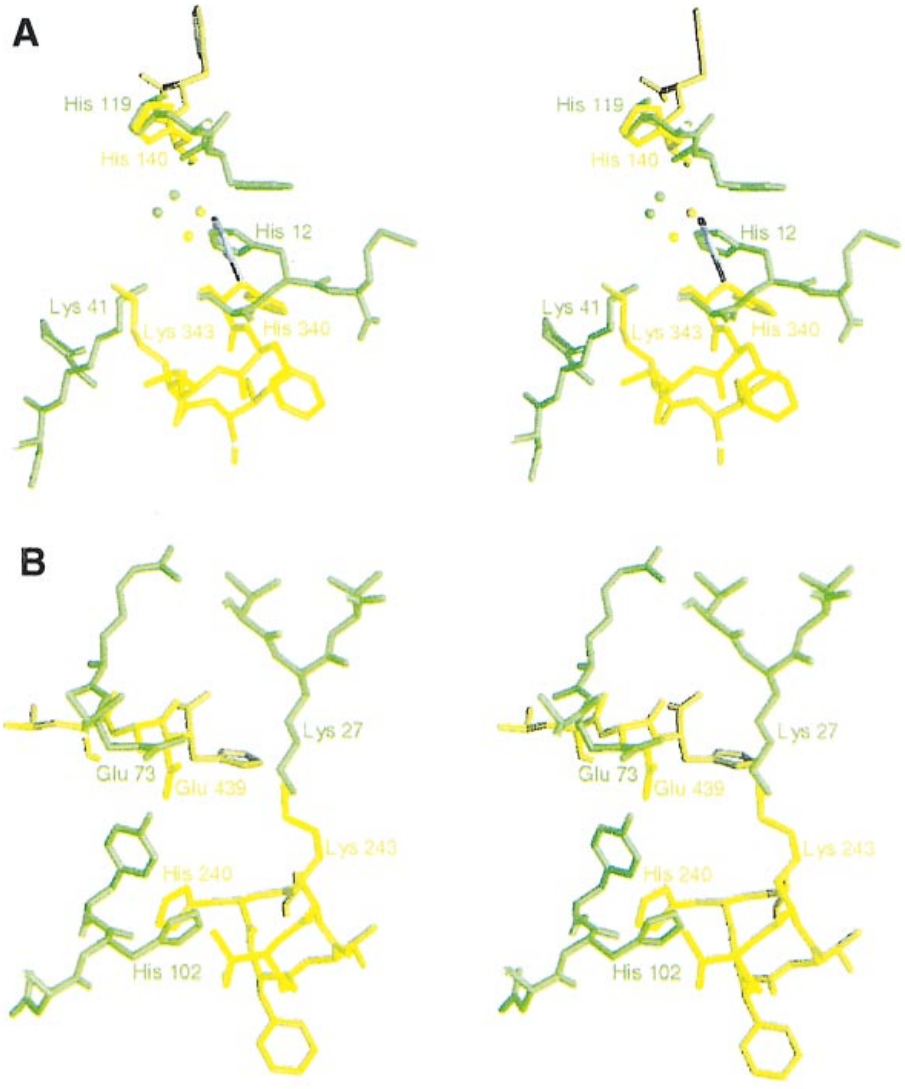

Fig. 5. (**A**) Superimposition of the active site of dimeric ImmE7 (M1 and M3, in yellow) on that of mammalian RNase A (in green). The residues His12, His119 and Lys41 of RNase A overlap with His340, His140 and Lys343 of dimeric ImmE7 at the same positions when the imidazole ring of His340 is rotated by ~120°. The rotated His340 is colored gray. Two water molecules, indicated by round spheres, are observed in the pocket of the active site of phosphate-free RNase and two water molecules were also found in the proposed active site of ImmE7. (**B**) Superimposition of the active site of dimeric ImmE7 (M2 and M4, in yellow) on that of microbial barnase (in green). The residues involved in the hydrolysis reaction in barnase, His102, Lys27 and Glu73, are located in the same region as His240, Lys243 and Glu439 of ImmE7. The two overlapping figures used two different dimer pairs (M1/M3 and M2/M4) to show that the geometry of the residues located at the proposed active sites in both of the dimers are similar.

codon (Figure 7A). pSE4R produced a translational stop site (UGA) located 29 nt downstream of the *ceiE7* stop codon. With isopropyl β-D-thiogalactoside (IPTG) induction, cells containing either pHK001-13R (in-frame fusion; Figure 7A) or pSE4R started to lyse 30 min after induction (Figure 7B), whereas cell lysis was not observed in cells carrying pHK001-14R upon IPTG induction. These results suggest that ribosome pausing at the translational stop codon of the *ceiE7* cistron may hinder formation of the T1 hairpin structure in such a way that binding of the ribosome to the Shine–Dalgano sequence of *celE7* is not interfered with and as a result translation of *celE7* is initiated (Figure 7B). In contrast, as in the case of pHK001-14R (Figure 7B), ribosome pausing occurs 88 nt upstream of the original termination codon and thus formation of the stem–loop structure in the T1 region is favored. As a result, this hairpin structure may block binding of the ribosome to the Shine–Dalgano sequence of *celE7* and thus translation of the *celE7* gene is impossible. Obviously, cleavage of the *ceiE7* transcript may have a similar effect in favoring formation of the T1 stem–loop structure. Consequently, translational coupling of *ceiE7* and *celE7* is disrupted.

Discussion

Both *in vivo* and *in vitro* evidence support the idea that ImmE7 may autoregulate the cleavage of its own mRNA. The crystal structure of dimeric ImmE7 shows that the possible RNase active site is located at the dimer interface. The cleavage event may induce decay of upstream mRNA and at the same time turn off translational expression of downstream *celE7*. The sequence specificity of this putative enzyme is unclear, but the specific cleavage site of

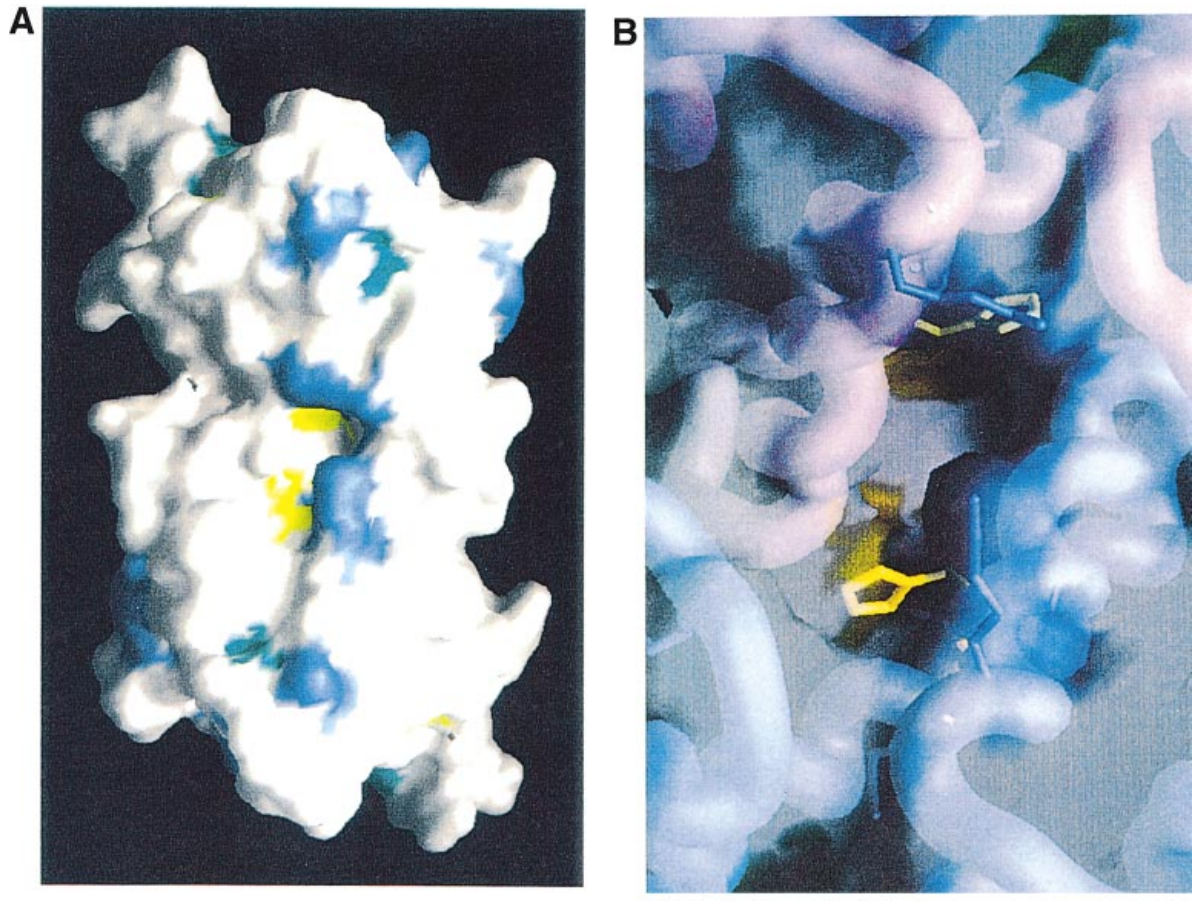

Fig. 6. (**A**) The molecular surface of ImmE7. The groove at the interface of dimeric ImmE7 between two adjacent Helices 2 was calculated by GRASP. This figure also displays the locations of the two histidines (His140 and His340) and all the basic residues (Lys and Arg). The surface histidine is colored yellow, lysine blue and arginine green. The basic residues are distributed along the groove and therefore could be responsible for docking the mRNA into the groove. (**B**) A close-up of the proposed RNase active site of dimeric ImmE7. The RNase active sites are located in a deep pocket in the middle of the groove in dimeric ImmE7. Residues His140, His340 and Lys343 are located on the surface of the central pocket and the two histidines, which are probably the general acid and base for the phosphodiester hydrolysis reaction, are located exactly above and beneath the pocket.

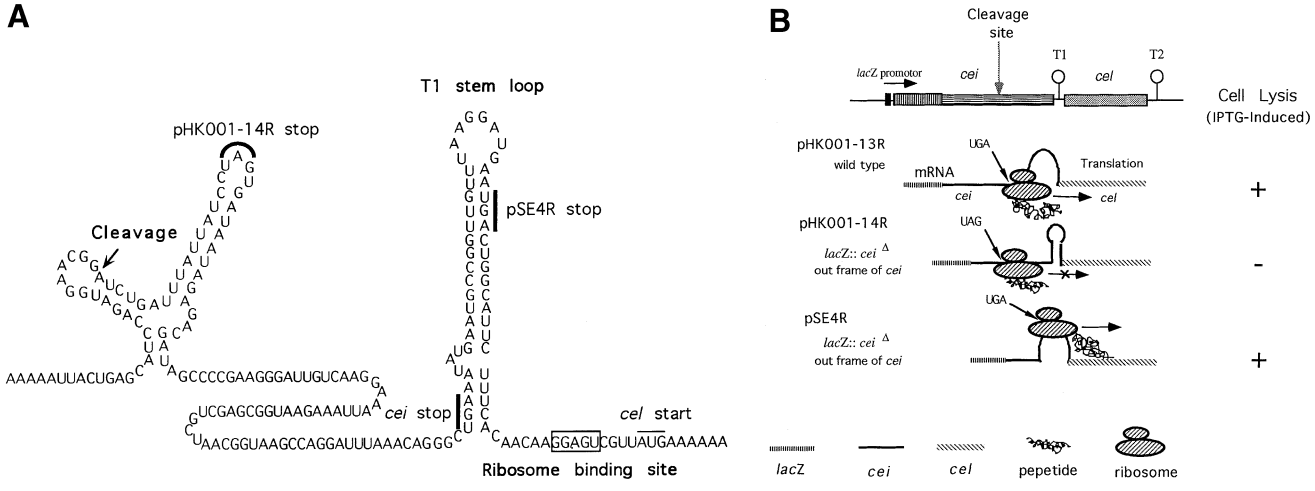

Fig. 7. Translational coupling of *ceiE7* and *celE7*. (**A**) Predicted secondary structure of the *ceiE7* mRNA showing the possible specific cleavage site and the T1 stem–loop structure. The arrow indicates the ImmE7-dependent cleavage site. Positions of the original stop codon, UGA, of *ceiE7* and the ribosome binding site, GGAGU, of *celE7* are indicated. Locations of the created stop signs (pHK001-14R and pSE4R) on the *cei–celE7* polycistronic transcript by out-of-frame translational fusion are also shown. (**B**) Schematic representation of the translational read-through from *ceiE7* to *celE7*. The genetic organization of the ColE7 operon (not to scale) is shown. The hypothetical position of the specific cleavage site on the *cei* gene is shown by a downward arrow. Positions of the two stem–loop structures (T1 and T2) of the operon are also shown. Horizontal arrows indicate either the direction of transcription or translation of recombinant plasmids pHK001-13R, pHK001-14R and pSE4R respectively. pHK001-14R and pSE4R are two out-of-frame fusions and pHK001-13R is an in-frame fusion. The effects of IPTG induction of *E.coli* strain JM109 harboring the corresponding recombinant plasmids are shown in the right hand panel. Cells were grown in LB medium to a OD_{600} of 0.2 and then IPTG was added to a final concentration of 20 μg/ml. + and –, cell lysis occurred or did not occur respectively after MMC induction.

ceiE7 mRNA has been identified and located in the proposed secondary structure (Figure 7A). Furthermore, ImmE7 protein is a multifunctional protein. It is well documented that this protein protects colicin-producing cells by inactivating colicin toxicity. The monomeric crystal structure of ImmE7 suggests that the highly negatively charged Helix-1–Loop–Helix-2 region of the protein may bind to the T2A domain of colicin (Ku *et al*., 1995; Chak *et al*., 1996) and as a result the DNase domain of colicin is inactivated. Translocation of colicins is coupled with that of its cognate immunity protein, suggesting that Imm protein may act as a chaperone-like substance to assist exportation of colicins through the membrane. Interestingly, cells containing the *ceiE7* gene are more resistant to low temperatures than host cells containing no *cei* gene (data not shown), suggesting that the functional targets of ImmE7 may be far broader than we previously expected.

Bovine seminal RNase, which belongs to the same superfamily as RNase A, is the only dimeric RNase isolated thus far (Piccoli *et al*., 1992). Two disulfides reinforce the non-covalent links between the two subunits. In the crystal structure of naturally dimerized seminal RNase, the two subunits swap their N-terminal segments and the composite active sites are made by residues from the two different subunits. The nature of these shared active sites is similar to that proposed for dimeric ImmE7. Rop protein, encoded by the ColE1 plasmid of *E.coli*, is another example of a dimeric RNA-binding protein (Predki *et al*., 1995). It binds hairpin pairs formed between RNA II and RNA I and regulates plasmid copy number. X-ray crystallographic studies (Banner *et al*., 1987) have shown that dimeric Rop forms a four helix bundle structure and a recent genetic analysis demonstrated that RNA binding determinants reside on one face of the protein formed by two helices (1 and 1′), one from each monomer. The residues form a thin stripe down the center of this face and it is suggested that the protein and RNA interact in a 'parallel' fashion. The central core of dimeric ImmE7 is similar to a four helix bundle structure and we suspect that RNA binds between the two Helices 2. The predicted secondary structure of the mRNA around the cleavage site is a hairpin structure. It is also possible that ImmE7 specifically recognizes this kind of RNA structure, similarly to Rop, the binding of which has been shown to be structure specific.

The proposed autoregulatory pathway of expression of the ColE7 operon controlled by ImmE7 is shown in Figure 8. The central theme of this autoregulation is the dynamic equilibrium between the monomeric and dimeric form of ImmE7. We propose that the function of monomeric ImmE7 is to inactivate colicin by binding to the T2A domain. In addition, dimeric ImmE7 exhibits a novel RNase activity and can be expected to regulate translational expression of the *cel* as well as the *cea* gene by specific cleavage of it own transcripts. *ceiE7* contains two constitutive promoters (Soong *et al*., 1994). Therefore, we hypothesize that expression of the *ceiE7* gene is independent of the SOS response promoter of the ColE7 operon. This speculation has been confirmed by Western blot analysis, which demonstrated that ImmE7 is at least 20 times in excess of colicin E7 (our unpublished data). Therefore, the amount of housekeeping ImmE7 protein is more than enough to protect cells from the toxic effects of either exogenous or endogenous colicin produced by basal level expression of the operon. If the amount of ColE7 polycistronic transcript increases substantially by overexpression from the inducible promoter, then a new state of dynamic equilibrium will be created, whereby more dimeric ImmE7 from the ImmE7 pool will be formed to cleave its own transcript. As a result, autoregulation of translational expression of the ColE7 operon will be achieved.

Delayed expression of the *cel* gene in response to induction of the SOS promoter (Lu and Chak, 1996) has been observed. This phenomenon can be explained by the presently proposed autoregulatory pathway. Excessive amounts of housekeeping dimeric ImmE7 may cleave the *cea–cei–cel* polycistronic transcripts at a specific site located in the *cei* gene, leading to uncoupling of translational expression (Figure 7B) of the *cel* gene. However, if induction of the SOS response promoter is sustained for 100 min, as in the case of the ColE7 operon (Lu and Chak, 1996), the amount of housekeeping dimeric ImmE7 is no longer sufficient to cope with the vastly increased numbers of *cea–cei–cel* polycistronic transcripts and, in this situation, overexpression of the *cel* gene would cause cell lysis.

It is known that translation influences the accessibility of endonuclease cleavage sites (Belasco and Higgins, 1988; Higgins *et al*., 1992). Pauses in polypeptide chain elongation have been reported to result from unusual codon usage for colicins (Varenne *et al*., 1982; Morlon *et al*., 1983). We have also observed that many non-optimal codons are used in *ceiE7* mRNA. This observation indicates that translational pausing may occur during translation of *cei* mRNA, thereby the formation of a specific mRNA secondary structure due to this translational pause may be susceptible to ribonucleolytic attack by dimeric ImmE7.

Oligonucleotide-directed site-specific mutagenesis of the *cei* gene has been carried out to investigate the actual binding site between ImmE7 and ColE7 protein, the interaction face for dimeric ImmE7 and the actual location of the putative RNase active site of ImmE7. We have also designed a set of experiments to locate the mRNA binding site of dimeric ImmE7. Moreover, co-crystallization of ImmE7 with ColE7 or RNA analogs is under investigation.

Materials and methods

Bacterial strains, plasmids and growth conditions

Escherichia coli W3110 (ColE7-K317) from the collection of Dr R.James (Chak *et al*., 1991) and *E.coli* W3110 and JM109 (Yanisch-Perron *et al*., 1985) were the hosts of the plasmids used in this study. *Escherichia coli* K12 isogenic strains N3433 (*lacZ*43, *rel*A, *spo*T1, *thi*1), N3431 (*rne*-3071ts), RS6521 (*rnc*::Tn*10*/Tet^r *rnc*$^-$) and SW001 (*rnc*::Tn*10*/ts (*rne*-3071) Tet^r *rnc*$^-$) were kindly provided by Dr Sue Lin-Chao. Plasmids pHK001-13R and pHK001-14R were constructed from derivatives of ExoIII-digested pHK001 (Soong *et al*., 1992). pHK001-13R contains the DNA fragment of *cei–cel* from nt –110 to the *Eco*RI site of pColE7 (the first nucleotide of the *cei*E7 start codon is defined as +1), while pHK001-14R and pSE4R include the sequence from +141 to the *Eco*RI site and +252 to the *Eco*RI site respectively. These three DNA fragments were cloned into pUC19. pYAN13R was as pHK001-13R except that the cloning vector was pGEM3Z(f). Bacteria were cultured in L broth. For selection or induction, ampicillin, IPTG and mitomycin C (MMC) were added to final concentrations of 100, 20 and 0.5 μg/ml respectively.

DNA and RNA techniques

Restriction enzymes, SP6 RNA polymerase, RNase-free DNase I, T4 polynucleotide kinase, M-MLV and retrotherm reverse transcriptases,

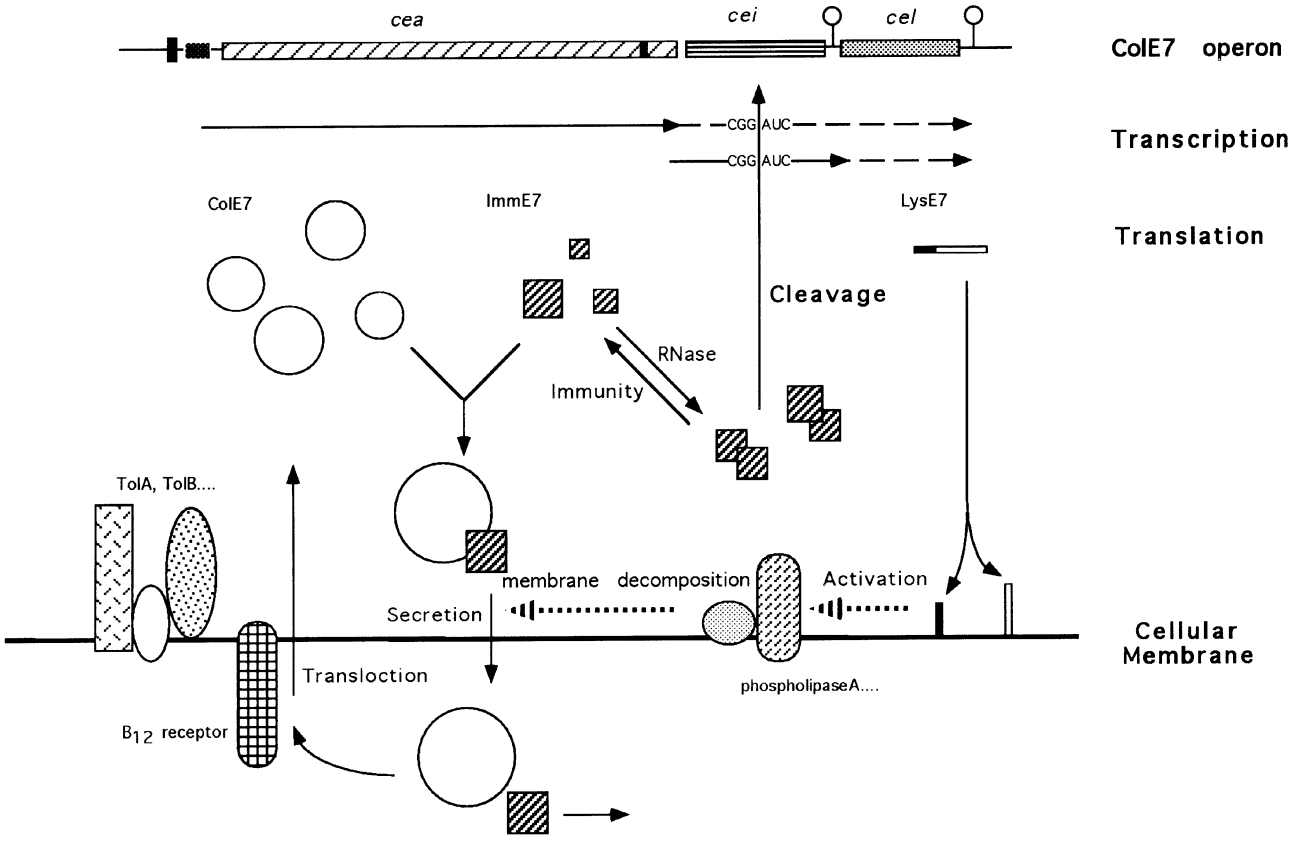

Fig. 8. Autoregulatory pathway for control of expression of the ColE7 operon. The amounts of monomeric and dimeric ImmE7 proteins *in vivo* are in a state of dynamic equilibrium. Monomeric ImmE7 inhibits the toxicity of colicin by binding to the T2A domain, whereas dimeric ImmE7 exhibits a specific RNase activity to control translational expression of the ColE7 operon. If induction of the SOS response promoter only lasts for a short time, the uncoupling of transcription and translation exerted by the ribonucleolytic activity of dimeric ImmE7 can keep the Lys proteins (*cel* gene product) well below the lethal dosage. Thereby cell integrity will be maintained. On the other hand, if induction of the SOS promoter lasts for an extended period, the amount of dimeric ImmE7 will not be adequate to keep the Lys proteins below the lethal threshold level and thereby cell lysis of the producing cell may occur. A detailed description of this autoregulatory pathway is provided in the Discussion section. A possible role of LysE7 in exportation of the Col–Imm complex is shown. TolA and TolB are the two outer membrane proteins involved in translocation of colicins. A schematic map of the ColE7 operon and the possible specific cleavage site of the *cei* transcript are also shown.

DNA sequenase and DNA ligase were purchased from BRL, Promega, Boehringer Mannhein or Epicentre Co. and were used according to the manufacturer's instructions. Plasmid isolation, restriction, ligation and transformation were carried out as described by Sambrook *et al*. (1989).

Isolation of total RNA, primer extension and RT–PCR

Total RNA was extracted from lysed cells by the hot phenol method as described by von Gabain *et al*. (1983). For induction, bacteria were grown to an OD_{600} of 0.4 in L broth before addition of MMC (0.5 μg/ml) or IPTG (20 μg/ml). Samples were withdrawn at different time points and total RNA extracted and analyzed by primer extension (Sambrook *et al*., 1989) or used as templates for RT–PCR amplification.

Oligonucleotide primers used in the experiment were as follows: P1, 5′-CTGGCTTACCGTTAGCAGC; P2, 5′-GACGACGGTGATACTGTCC; P4, 5′-GACTTAGGTTCTCCTGTTCC; P5, 5′-CTAACACATCATCA-GT; PB, 5′-CCACCTGTGTTATGTGCGCC.

RT–PCR was performed at 94°C for 1 mim, 40°C for 5 min and 70°C for 10 mim for the first cycle and at 94°C for 1 min, 45°C for 75 s and 70°C for 2 min for another 30 cycles.

Preparation of crude extracts and purification of ColE7 and ImmE7

Preparation of S-30 extracts was according to the method described by Mackie (1991). Purification of ColE7 and ImmE7 were as described previously (Chak *et al*., 1991; Ku *et al*., 1995).

Assay of RNase activity and in vitro transcription

RNase activity assays were performed as described by Mackie (1991). *In vitro* transcription of *ceiE7* was carried out using SP6 RNA polymerase with a linear DNA template containing the *cei* gene. The detailed procedure was as described previously by Melton *et al*. (1984).

X-ray data collection and processing

Single monoclinic crystals were grown at room temperature by the sitting-drop vapor diffusion method from ammonium phosphate solution as described earlier (Ku *et al*., 1995). X-ray diffraction data were collected using an R-AXIS II image plate detector equipped with a Rigaku RU-300 generator operating at 50 kV and 80 mA. The data collected on a single monoclinic crystal at room temperature were processed using RAXIS software. Detailed statistics for the native data are listed in Table I.

Structure determination

The monoclinic crystal form of ImmE7 belongs to space group $P2_1$. Calculations of self-rotation maps at different resolution ranges using XPLOR (Brunger, 1992) yielded prominent peaks for two non-crystallographic dyads in the directions of the *a*- and *c*-axes, corresponding to spherical angles of $\psi = 90°$ and $\phi = 0$ and 90° respectively. The refined structure from the orthorhombic I222 crystal was employed as a search model in a cross-rotational search. Several different resolution limits, ranging from 5 to 2.5 Å, were used in the rotation function calculations. The rotation function searches yielded 150–200 highest peaks, which were then subjected to filtering by PC refinement procedures in XPLOR. No straightforward solution was obtained from a single search, but among the peak positions with the highest PC values, four sets of angles were extracted by comparing results from different resolution ranges. These angles persistently appeared at the top of the lists and represented four possible orientations of ImmE7 molecules in the monoclinic unit

cell. They are (θ_1, θ_2, θ_3) = (65.5°, 66.5°, 97.5°), (66.5°, 63.0°, 273.5°), (228.0°, 73.0°, 159.5°) and (238.5°, 77.0°, 333.5°). We noticed that the first orientation (M1) is related to the second (M2) and the third (M3) is related to the fourth (M4) by a non-crystallographic 2-fold symmetry that is almost parallel to the *c*-axis.

The translational function search was divided into two parts: (i) a search in the *a*–*c* plane for each of the four ImmE7 molecules; (ii) a search along the *b*-axis for relative positions between the molecules. To carry out (i), different resolution ranges were tested to produce a clearly interpretable map for each molecule. Four major peaks at (*x*, *z*) = (0.188, 0.094) for M1, (0.281, 0.094) for M2, (0.483, 0.047) for M3 and (0.031, 0.063) for M4 were found. For the translational search (ii), diffraction data between 12 and 3 Å resolution with $F/\sigma > 3$ were used in the calculation of intermolecular translation functions in which M1 was fixed at the origin while M2, M3 or M4 was moved along the *b*-axis. A unique peak was observed for M2 at $y = 0.789$, with the addition of the half-lattice vector (0, 0, 1/2); for M3 it was at $y = 0.031$ with vector (1/2, 0, 1/2); for M4, $y = 0.750$ with vector (1/2, 0, 0). Highly consistent results were obtained with one of the other three molecules fixed and these reconfirmed the disposition of ImmE7 molecules in the monoclinic unit cell.

The N-terminus of M1 was in poor contact with Helix 2 of M3 near residue 36 in the starting model. The N-terminus of M3 was also in contact with Helix 2 of M1, again near residue 36. Similar relationships were observed between M2 and M4. In spite of the N-terminus and Helix 2 being in poor contact, no other parts of the protein molecules interacted unfavorably with its neighbors. Rigid-body refinement of the four molecules against 19 710 reflections between 20 and 2 Å resolution with $F/\sigma > 2$ yielded an *R* value of 0.42. The N-terminal residue Leu3 was displaced by 5 Å, because there were densities corresponding to this new position, and relieved the poor contact with Helix 2 of its neighbor. There were also densities in the adjacent regions for possible extension towards the two terminal residues Met1 and Glu2, which were not observed in the orthorhombic crystal. The conformations of the N-terminal strands were similar but not identical in all four cases. The final model consists of four polypeptide chains, in which the residues were numbered 101–187, 201–287, 301–387 and 401–487, and 127 water molecules. With 8% of data reserved for R_{free}, the *R* factor is 18.4% and R_{free} is 26.8 %, using a total of 24 783 reflections with $F > 2\,\sigma(F)$ in the 6.0–1.8 Å resolution shell.

Acknowlegements

This work was support by the Academia Sinica and National Science Council (NSC) of the Republic of China with grants to K.-F.C. (NSC85-2331-B010-105 and NSC86-2314-B010-011) and H.S.Y. (NSC86-2313-B001-005).

References

Banner,D.W., Kokkinidis,M. and Tsernoglou,D. (1987) Structure of the ColE1 rop protein at 1.7 Å resolution. *J. Mol. Biol*., **196**, 657–679.

Belasco,J.G. and Higgins,C.F. (1988) Mechanisms of mRNA decays in bacteria: a perspective. *Gene*, **72**, 15–23.

Bowman,C.M., Dahlberg,J.E., Ikemura,T., Konisky,J. and Normra,M. (1971) Specific inactivation of 16S ribosomal RNA induced by colicin E3 *in vivo*. *Proc. Natl Acad. Sci. USA*, **68**, 964–968.

Brunger,A.T. (1992) *X-PLOR, Version 3.1: A System for X-ray Crystallography and NMR*. Yale University Press, New Haven, CT.

Campbell,R.L. and Petsko,G.A. (1987) Ribonuclease structure and catalysis: crystal structure of sulfate-free native ribonuclease A at 1.5 Å resolution. *Biochemistry*, **26**, 8579–8584.

Chak,K.-F. and James,R. (1985) Analysis of the promoters for the two immunity genes present in the ColE3-CA38 using two new promoter probe vectors. *Nucleic Acids Res*., **7**, 2519–2531.

Chak,K.-F., Kuo,W.-S., Lu,F.-M. and James,R. (1991) Cloning and characterization of the ColE7 plasmid. *J. Gen. Microbiol*., **137**, 91–100.

Chak,K.-F., Safo,M.K., Ku,W.-Y., Hsieh,S.-Y. and Yuan,H.S. (1996) The crystal structure of the ImmE7 protein suggests a possible colicin-interacting surface. *Proc. Natl Acad. Sci. USA*, **93**, 6437–6442.

Cooper,P.C. and James,R. (1984) Two new E colicins, E8 and E9, produced by a strain of *Escherichia coli*. *J. Gen. Microbiol*., **130**, 209–215.

DiMasi,R.D., White,J.C., Schnaitman,C.A. and Bradbeer,C. (1973) Transport of vitamin B12 in *E. coli*: common receptor sites for vitamin B12 and the E colicins on the outer membrane of the cell envelope. *J. Bacteriol*., **115**, 506–573.

Herschman,H.R. and Helinski,D.R. (1967) Comparative study of the events associated with colicin induction. *J. Bacteriol*., **94**, 691–699.

Higgins,C.F., Peltz,S.W. and Jacobson,A. (1992) Turnover of mRNA in prokaryotes and lower eukaryotes. *Curr. Opin. Genet. Dev.*, **2**, 739–747.

Janin,J., Miller,S. and Chothia,C. (1988) Surface, subunit interfaces and interior of oligomeric proteins. *J. Mol. Biol*., **204**, 155–164.

Jensen,R.B. and Gerdes,K. (1995) Programmed cell death in bacteria: proteic plasmid stabilization systems. *Mol. Microbiol*., **17**, 205–210.

Koepke,J., Maslowska,M., Heinemann,U. and Saenger,W. (1989) Three-dimensional structure of ribonuclease T1 complexed with guanyly-2′,5′-guanosine at 1.8 Å resolution. *J. Mol. Biol*., **206**, 474–488.

Kraulis,P.J. (1991) MOLSCRIPT: a program to produce both detailed and schematic plots of protein structures. *J. Appl. Crystallogr.*, **24**, 946–950.

Ku,W.-Y., Wang,C.-S., Chen,C.-Y., Chak,K.-F., Safo,M.K. and Yuan,H.S. (1995) Crystallization and preliminary x-ray crystallographic analysis of ImmE7 protein of colicin E7. *Proteins Struct. Funct. Genet*., **23**, 588–590.

Kurihara,H., Mitsui,Y., Ohgi,K., Irie,M., Mizuno,H. and Nakamura,K.T. (1992) Crystal and molecular structure of RNase Rh, a new class of microbial ribonuclease from *Rhizopus niveus*. *FEBS Lett*., **306**, 189–192.

Laskowski,R.A., MacArthur,M.W., Moss,D.S. and Thornton,J.M. (1993) PROCHECK: a program to check the stereochemical quality of protein structures. *J. Appl. Crystallogr*., **26**, 283–291.

Little,J.W. and Mount,D.W. (1982) The SOS regulatory system of *Escherichia coli*. *Cell*, **29**, 11–12.

Lu,F.-M. and Chak,K.-F. (1996) Two overlapping SOS-boxes in ColE operons are responsible for the viability of cells harboring the Col plasmid. *Mol. Gen. Genet*., **251**, 407–411.

Mackie,G.A. (1991) Specific endonucleolytic cleavage of the mRNA for ribosomal protein S20 of *Escherichia coli* requires the product of the *ams* gene *in vivo* and *in vitro*. *J. Bacteriol*., **173**, 2488–2497.

Matthews,B.W. (1968) Solvent content of protein crystal. *J. Mol. Biol*., **33**, 491–497.

Mauguen,Y., Hartley,R.W., Dodson,E.J., Dodson,G.G., Bricogne,G., Chothia,C. and Jack,A. (1982) Molecular structure of a new family of ribonucleases. *Nature*, **297**, 162–164.

Melton,D.A., Krieg,P.A., Rebagliatte,M.R., Maniatis,T., Zinn,K. and Green,M.R. (1984) Efficient *in vitro* synthesis of biologically active RNA and RNA hybridization probes from plasmids containing a bacteriophage SP6 promoter. *Nucleic Acids Res*., **12**, 7035–7065.

Morlon,J., Lloubes,R., Varnne,S., Chartier,M. and Lazdunski,C. (1983) Complete nucleotide sequence of the structural gene for colicin A, a gene translated at non-uniform rate. *J. Mol. Biol*., **170**, 271–285.

Nachman,J., Miller,M., Gilliland,G.L., Carty,R., Pincus,M. and Wlodawer,A. (1990) Crystal structure of two covalent nucleoside derivatives of ribonuclease A. *Biochemistry*, **29**, 928–937.

Nicholls,A. and Honig,B. (1991) A rapid finite difference algorithm, utilising successive over relaxation to solve the Poisson–Boltzmann equation. *J. Comp. Chem*., **12**, 435–445.

Nonaka,T., Nakamura,K.T., Uesugi,S., Ikehara,M., Irie,M. and Mitsui,Y. (1993) Crystal structure of ribonuclease Ms (as a ribonuclease T1 homologue) complexed with a guanylyl-3′,5′-cytidine analogue. *Biochemistry*, **32**, 11825–11837.

Piccoli,R., Tamburrini,M., Piccialli,G., Di Donato,A., Parente,A. and D'Alessio,G. (1992) The dual-mode quaternary structure of seminal RNase. *Proc. Natl Acad. Sci. USA*, **89**, 1870–1874.

Predki,P.F., Nayak,M., Gottlieb,M.C. and Regan,L. (1995) Dissecting RNA–protein interactions: RNA–RNA recognition by Rop. *Cell*, **80**, 41–50.

Pugsley,A.P. and Schwartz,M. (1984) Colicin E2 release: lysis, leakage or secretion? Possible role of a phospholipase. *EMBO J*., **3**, 2393–2397.

Ramakrishnan,C. and Ramachandran,G.N. (1965) Stereochemical criteria for polypeptide and protein chain conformation. *Biophys. J*., **5**, 909–933.

Sambrook,J., Fritsch,E.F. and Maniatis,T.M. (1989) *Molecular Cloning: A Laboratory Manual*, 2nd edn. Cold Spring Harbor Laboratroy Press, Cold Spring Harbor, NY.

Schaller,K. and Nomura,M. (1976) Colicin E2 is a DNA endonuclease. *Proc. Natl Acad. Sci. USA*, **68**, 3989–3993.

Sevcik,J., Dodson,E.J. and Dodson,G.G. (1991) Determination and restrained least-squares refinement of the structures of ribonuclease Sa and its complex with 3′-guanylic acid at 1.8 Å resolution. *Acta Crystallogr*., **B47**, 240–253.

Soong,B.-W., Lu,F.-M. and Chak,K.-F. (1992) Characterization of the *cea* gene of the ColE7 plasmid. *Mol. Gen. Genet*., **233**, 177–183.

Soong,B.-W., Hsieh,S.-Y. and Chak,K.-F. (1994) Mapping of initiation start sites of the *cea* and *cei* genes of the ColE7 plasmid. *Mol. Gen. Genet*., **243**, 477–481.

Toba,M., Masaki,H. and Ohta,T. (1988) Colicin E8, a DNase which indicates an evolutionary relationship between colicins E2 and E3. *J. Bacteriol*., **170**, 3237–3242.

Tokuda,H. and Konisky,J. (1979) Effect of colicins Ia and E1 on ion permeability of liposomes. *Proc. Natl Acad. Sci. USA*, **76**, 6167–6171.

Varenne,S., Knibiehler,M., Cavard,D., Morlon,J. and Lazdunski,C. (1982) Variable rate of polypeptide chain elongation for colicin A, E2 and E3. *J. Mol. Biol*., **159**, 57–70.

Vassylyev,D.G. *et al.* (1993) Crystal structure of ribonuclease F1 of *Fusarium moniliforme* in its free form and in complex with 2′GMP. *J. Mol. Biol*., **230**, 979–996.

von Gabain,A., Belasco,J.G., Schottel,J.L. and Chang,C.Y. (1983) Decay of mRNA *in E. coli*: investigation of the fate of specific segments of transcripts. *Proc. Natl Acad. Sci. USA*, **80**, 653–657.

Wallis,R., Leung,K.-Y., Pommer,A.J., Videler,H., Moore,G.R., James,R. and Kleanthous,C. (1995a) Protein–protein interactions in colicin E9 DNase–immunity protein complexes. 2. Cognate and noncognate interactions that span the millimolar to femtomolar affinity range. *Biochemistry*, **34**, 13751–13759.

Wallis,R., Moore,G.R., James,R. and Kleanthous,C. (1995b) Protein–protein interactions in colicin E9 DNase–immunity protein complexes. 1. Diffusion-controlled association and femtomolar binding for the cognate complex. *Biochemistry*, **34**, 13743–13750.

Watson,R., Rowsome,W., Tsao,J. and Visentin,L.P. (1981) Identification and characterization of Col plasmids from classical colicin E-producing strains. *J. Bacteriol*., **147**, 569–577.

Wlodawer,A., Svensson,L.A., Sjolin,L. and Gilliland,G.L. (1988) Structure of phosphate-free ribonuclease A refined at 1.26 Å. *Biochemistry*, **27**, 2705–2717.

Wodak,S.Y., Liu,M.Y. and Wyckoff,H.W. (1977) The structure of cytidilyl(2′,5′)adenosine when bound to pancreatic ribonuclease S. *J. Mol. Biol*., **116**, 855–875.

Yanisch-Perron,C., Vieira,J. and Messing,J. (1985) Improved M13 phage cloning vectors and host strains: nucleotide sequences of the M13mp18 and pUC19 vectors. *Gene*, **33**, 103–119.

Yarmolinsky,M.B. (1995) Programmed cell death in bacterial populations. *Science*, **267**, 836–837.

Zegers,I., Maes,D., Dao-Thi,M.-H., Poortmans,F., Palmer,R. and Wyns,L. (1994) The structure of RNase A complexed with 3′-CMP and d(CpA): active site conformation and conserved water molecules. *Protein Sci*., **3**, 2322–2339.

Received on July 22, 1996; revised on October 11, 1996